Fracture Mechanics of Concrete and Concrete Structures -
High Performance, Fiber Reinforced Concrete, Special Loadings and Structural Applications- B. H. Oh, et al. (eds)

Methodology of modeling fiber reinforcement in concrete elements

P. Stroeven
Faculty of Civil Engineering and Geosciences, Delft University of Technology the Netherlands

ABSTRACT: This paper's focus is on the modeling methodology of (steel) fiber reinforcement in concrete. The orthogonal values of fiber efficiency are presented. Bulk as well as boundary situations are covered. Fiber structure is assumed due to external compaction by vibration to display a partially linear planar structure (Stroeven-concept), which can even be simplified in many practical situations to a partially planar system. The two unknown parameters can be experimentally assessed in a single vertical projection image by orthogonal line scanning. Several boundary conditions are distinguished and the practical case of a thin SFRC plate is evaluated. Advantages over a practical but very approximate proposal in the open literature are shown.

1 INTRODUCTION

Mechanical and fracture mechanical properties of steel fiber reinforced concrete (SFRC) elements will partly depend on the reinforcement characteristics. Isotropic uniform randomness (IUR) of fiber dispersion is generally assumed in design; however, laboratory research revealed significant deviations of this "ideal" state, which is mainly due to compaction by vibration; a phenomenon that is now widely acknowledged. Moreover, boundaries additionally influence the reinforcing effect. Both phenomena have inevitable impact on (fracture) mechanical behavior.

A practical and economic concept for modeling fiber dispersion is based on the partially linear-planar reinforcement system (the so called "Stroe-ven-concept"). This renders possible experimental assessment of actual 3D dispersion characteristics of fibers on an ortrip (orthogonal tripod) sampling scheme. For simple loading situations, this can even be simplified into a so called vertical sectioning scheme. The underlying geometrical statistical framework has been extensively described in the literature (Stroeven 2009).

The boundary case can be approached by similar geometrical statistical modeling. In the literature, this methodology is outlined for a declining fiber density in boundary layers as found in at least part of the experiments using external vibration (Stroeven & Hu 2006). Internal vibration may have influence on bulk and boundary disturbance of fibers (Gettu et al. 2005). Since also increases in fiber density are sometimes observed in boundary layers, this methodology based on the partially linear-planar concept is rejected as irrelevant or incorrect. However, the methodology is correct; instead, the geometrical statistical assumptions underlying modeling of fiber dispersion should be adapted to the actual situation in this methodological approach. Basically, any situation encountered in the real material can be properly modeled in the aforementioned methodology. This also involves the various boundary situations that can arise in full-scale structures or in laboratory research. This will influence, of course, global (fracture) mechanical properties of SFRC elements. The paper does not pursue presenting all published analytical work. Instead, ultimate goal of the paper is demonstrating that the problem of steel fiber reinforcement in bulk and at boundaries can be approached analytically, so that it is unnecessary to accept an intuitive but arbitrary solution, as sometimes proposed in the literature (Soroushian & Lee 1990a).

Performance characteristics of SFRC are formulated by a law of mixtures concept in which a matrix contribution and one due to the reinforcement of short dispersed fibers. The latter is governed by the so called fiber factor, which is the product of fiber volume fraction V_f, fiber aspect ratio $a=l/d$ (l and d are fiber length and diameter, respectively) and steel-matrix interfacial friction τ_f (Yamada & Ishiyama 2004). Non-alignment of fibers and stresses leads to a reduced efficiency for stress transfer expressed by a global efficiency factor for stress transfer η (Stroeven 2009, Stroeven & Hu 2006, Bonzel & Schmidt 1985, Bentur & Mindess 1990). This paper will deal with η under various conditions.

2 BULK FIBER EFFICIENCY

In a SFRC composite with anisometry in fiber reinforcement, we have anisotropy in composite strength that can be expressed by law of mixtures relationships:

$$\sigma(x) = \sigma_m(1-V_f) + \eta(x)a\tau_f V_f$$
$$\sigma(y) = \sigma_m(1-V_f) + \eta(y)a\tau_f V_f \quad (1)$$
$$\sigma(z) = \sigma_m(1-V_f) + \eta(z)a\tau_f V_f$$

in which σ_m stands for the tensile strength of the plain mortar, and $\sigma(x)$, $\sigma(y)$ and $\sigma(z)$ are the orthogonal strength components due to the dispersed fibers in the concrete.

The fresh mixture of SFRC is assumed compacted in a prismatic mould in the direction of the *z*-axis of a Cartesian co-ordinate system $\{x,y,z\}$. The longitudinal axis coincides with the *x*-axis of this co-ordinate system. The situation is shown in Figure 1.

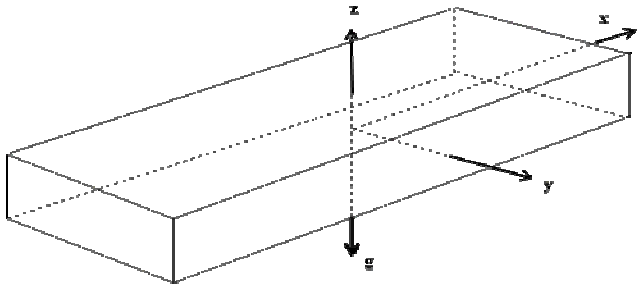

Figure 1. SFRC specimen compacted in the direction of the z-axis of the Cartesian coordinate system $\{x,y,z\}$. *g* indicates the gravitation force during compaction.

This paper will derive estimates for the efficiency factors, $\eta(x)$, $\eta(y)$, and $\eta(z)$, to be associated with fiber contributions to tensile strength characteristics in the respective coordinate directions. The most general case of dispersed fibers can be modeled on global (engineering) level according to Stroeven by a so-called partially linear-planar fiber system (Stroeven 1979a,b, Stroeven 2009, Stroeven & Hu 2006). The underlying assumption leads to quite accurate results, and greatly simplifies experimental approaches, because random sampling, necessary for obtaining unbiased three-dimensional structural information, can be avoided. So, this assumption has significant economic implications.

Major advantage of the model is that we can concentrate on the different fiber portions separately. It implies the linear fiber fraction, L_V (=L/V, total fiber length, L, per unit volume, V), to be partly composed of an isotropic uniform random (IUR) portion, L_{V3}. To it is added a portion of fibers that are parallel to an orientation plane (which is in concrete practice perpendicular to the compaction direction), but otherwise distributed two-dimensionally uniformly random as to the location of their centers, L_{V2}. Finally, a portion is added in which all fibers are parallel to an orientation axis (mostly, the axis of an elongated SFRC specimen), but with otherwise uniform random distribution of their centers, L_{V1}. These fiber portions are in this paper attributed as the 3D, 2D and 1D ones. They contribute all three to the reinforcement in the *x*-direction in Figure 1, whereas only the 3D and 2D portions contribute to the reinforcement in the *y*-direction. Finally, only the 3D portion contributes to fiber reinforcement in the *z*-direction.

In design it is assumed that $L_{V1} = L_{V2} = 0$, so that only a single efficiency factor is resulting; it is said that the fibers are "randomly" (more precisely: IUR) distributed in this case. However, only the fibers intersecting the leading crack (constituting the so-called active portion) can contribute to global stress transfer. In this hypothetical situation (of IUR fiber reinforcement in bulk), only 50% of the fibers in the neighborhood of the leading crack are activated (Stroeven 1989), and their orientation distribution is far from IUR (Stroeven 2009, Bentur & Mindess 1990, Bayard et al 2004). Estimation of the fiber efficiency parameters in this paper is therefore solely based on the active fiber portion.

Basis of all analytical expressions is the intersection of a fiber and a (supposedly) flat crack. The probability for such an event depends on the tangent height (or projected length) of the fiber perpendicular to the crack. This is proportional to $\cos\theta$ in Figure 2**.** The L_{V3} system has a number of fibers proportional to $\sin\theta$ oriented similarly with respect to the crack plane. This is a factor mostly missing in similar approaches; however they should all be included in an analytical approach to deriving fiber efficiency of the 3D IUR portion (Stroeven 2009, Stroeven & Hu 2006). Note that $\overline{e}_i = l/4$.

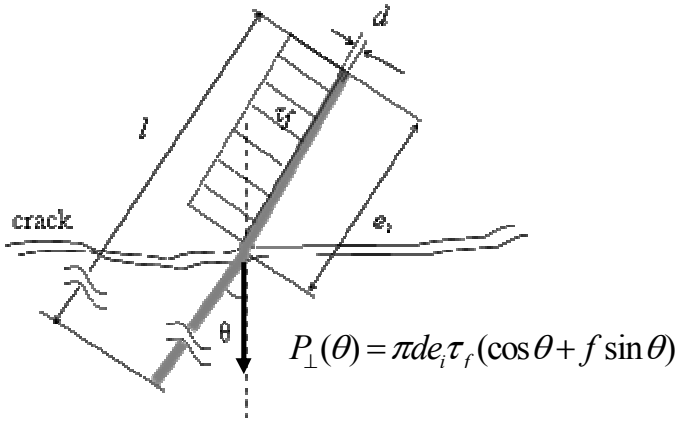

Figure 2. Steel fiber intersecting a crack in concrete transfers a load $P_\perp(\theta)$ perpendicular to the crack plane.

Geometric averaging of the expression for the load in Figure 2 for the 3D IUR portion only, yields

$$\overline{P}_{3\perp} = \frac{1}{6}\pi dl\tau_f(1+f) \quad (2)$$

By multiplying equation (2) with the number of fibers intersecting the crack per unit of area (NA), the stress transferred perpendicular to the crack is obtained. With $N_{A3} = (2V_{f3})/(\pi d^2)$ we obtain

$$\sigma_{\perp 3} = \sigma_3(x) = \sigma_3(y) = \sigma_3(z) = \frac{1}{3} a V_{f3} \tau_f (1 + f) \qquad (3)$$

In equations (2) and (3) and Figure 2, f is the friction resistance of the crack sheared over the crack edge. So, pull-out resistance and shearing over the crack edge are considered as contributing to load transfer over the crack. Here we have used mono-size fibers with circular cross section; however fibers with artificial shape can be treated along the same lines (Stroeven 2008, 2009).

Operating similarly for the 2D and 1D fiber portions, it is found that

$$\sigma_2(x) = \sigma_2(y) = \frac{1}{2} a V_{f2} \tau_f (1 + \frac{2}{\pi} f) \quad \text{and}$$
$$\sigma_2(z) = 0 \qquad (4)$$

$$\sigma_1(x) = a V_{f1} \tau_f \quad \text{and}$$
$$\sigma_1(y) = \sigma_1(z) = 0 \qquad (5)$$

Note that $V_{f1} + V_{f2} + V_{f3} = 1$. Finally, equations (3-5) yield for the efficiency factors in equation (1)

$$\eta(x) = \frac{1}{3}(1 + f)\frac{V_{f3}}{V_f} + \frac{1}{2}(1 + \frac{2}{\pi} f)\frac{V_{f2}}{V_f} + \frac{V_{f1}}{V_f} \qquad (6)$$

$$\eta(y) = \frac{1}{3}(1 + f)\frac{V_{f3}}{V_f} + \frac{1}{2}(1 + \frac{2}{\pi} f)\frac{V_{f2}}{V_f} \qquad (7)$$

$$\eta(z) = \frac{1}{3}(1 + f)\frac{V_{f3}}{V_f} \qquad (8)$$

Since the 3D IUR portion is considered the "normal" one, and generally the only one taken into account in the design stage, the other two are sometimes referred to as parasitic ones. One may substitute $V_{f2}/V_f = \omega_2$ and $V_{f1}/V_f = \omega_1$ in equations (6-8), whereby ω_2 and ω_1 are referred to as the planar and linear degree of orientation, respectively. Obviously, the aforementioned design value of fiber efficiency is 1/3. The expressions in equations (6-8) can lead to quite different outcomes, however. In Aveston & Kelly (1973), an example is presented for a partially linear system (with ω_1=0), whereby a realistic value of 0.25 is taken for ω_2 (see e.g., Stroeven & Shah (1978) from which Figure 3 is selected). It is shown that $\eta(z)$ for the pull-out mechanism only and $\eta(x)$ for the two mechanisms discussed herein will differ by a factor 2! Accounting for ω_1 may lead to even more dramatic differences and deviations from the design value.

Figure 3. X-ray radiograph of vertical slice of SFRC subjected to superimposed orthogonal grid for counting intersections with fiber projections (Stroeven & Shah 1978). The results obtained showed the fiber structure to reveal partially linear planar orientation; the compaction by vibration-induced reorientation in horizontal direction and the influence of the sides of the mould are obvious.

2.1 *Bulk fiber case for partially planar orientation*

The linear parasitic component is in many cases small enough to be neglected with respect to the planar one. Substitution of ω_1=0 in equations (6)-(8) yields

$$\eta(x) = \eta(y) \cong \frac{1}{3}(1 + f + \frac{1}{2}\omega_2) \qquad (9)$$

$$\eta(z) = \frac{1}{3}(1 + f)(1 - \omega_2) \qquad (10)$$

The degree of fiber anisometry, Ω, can be defined by

$$\Omega = \frac{\eta(x) - \eta(z)}{\eta(\omega_2 = 0)} = \frac{3}{2}\omega_2 \frac{1 + \frac{2}{3} f}{1 + f} \qquad (11)$$

Hence, Ω=0 defines an isometric fiber structure (that yields isotropic contributions to mechanical performance). Equation (21) reveals a maximum value of about 1.5 for the degree of anisometry. Further, it demonstrates that Ω and ω_2 are linearly dependent.

2.2 *Consequences for experimental assessment*

Equations (9) and (10) contain as unknown parameter only the degree of orientation that is composed, however, of two fiber portions, V_{f2} and V_f (so, V_{f3}). Hence, two independent observations would be required for the assessment of the two fiber portions in the practical situation of the partially planar case. It has been demonstrated elsewhere that observations by orthogonal line scanning on a so called vertical projection (*i.e.*, perpendicular to the orientation plane) suffices. Hence, 3D information is obtained by just sawing one (or more parallel) slice(s) from elements (see Fig. 3). A very significant reduction in efforts as compared to the earlier mentioned ortrip sampling. The reduction is of dramatic proportions as compared to random sampling that is generally required when confronted with anisotropic structures. Assumption of the "Stroeven" concept

constitutes a way out, so that this unpractical and laborious work can be avoided.

3 FIBER EFFICIENCY AT BOUNDARIES

To evaluate reinforcement situations at boundaries, we will employ the "unit" sphere model (Stroeven 2009, Stroeven & Hu 2006). This contains all fibers oriented as in the material and fixed with one end in the center. For mono-size fibers the other end covers the surface of the sphere. When isotropic uniformly random dispersed in bulk, coverage of the fiber ends is also uniformly random. Note that this does not necessarily require the fibers physically to be mono-size or straight. In complicated cases they may be hypothetically subdivided in mono-size straight sticks, which will replace the fibers in the sphere.

A similar approach can be used for visualization of fiber dispersion in the boundary zones. The boundary layer is hypothetically sectioned for this purpose, yielding a set of serial slices with thickness Δt parallel to the outer surface. The *t*-axis has its origin at this outer surface, and is perpendicular to it while pointing inward along the leading crack plane. In the present case, the sectioning is perpendicular to the *x*-axis. The leading crack is supposed flat and parallel to the {*x,y*}- plane. As a consequence, the tensile loading is in the *z*-direction. The situation is sketched in Figure 4 (Stroeven & Hu 2006). The smaller *t*, the larger the cut-off part of the sphere: fibers with their second end supposedly on the cut-off part of the sphere surface violate the boundary condition, because they would intersect with the mould. This situation is of geometric probability nature. To obtain reinforcement efficiency perpendicular to the crack, we need global geometric averaging over all possible fibers accounting for their orientation. Here, two ways can be defined:

1) all fibers intersecting the cut-off area are rejected; physically they cannot exist. Consequence is that the number of fibers declines on approach of the mould; on average they are more favorably oriented with respect to the crack thereby somewhat compensating for the number decline. However, a global reinforcement efficiency decline upon approach of the mold can be expected.

2) the rejected fibers are supposedly re-generated. Result is that the number of fibers is constant upon approach of the mould. The orientation effect is similar as in model 1). So, this will lead to fiber reinforcement efficiency to increase upon approach of the boundary.

We have some experimental evidence for model 1) (Stroeven & Babut 1986). Moreover, it is the more complicated one, because number of fibers and their orientation distribution will jointly change upon approach of the mold. In model 2) only orientation modifications should be accounted for, which are identical to those in model 1). Outcomes of model 2) can therefore be obtained following the same procedure as outlined *in detail* in the open literature [2]; the procedures are based on proper *geometrical statistical* interpretation of Figure 4, whereby the following trigonometric terms should at least be incorporated:

- *cosine term*, expressing the load component to be perpendicular to the crack;
- *cosine term*, representing the relative probability of fiber intersecting with the crack;
- *sine term*, being the relative spatial frequency of the fibers

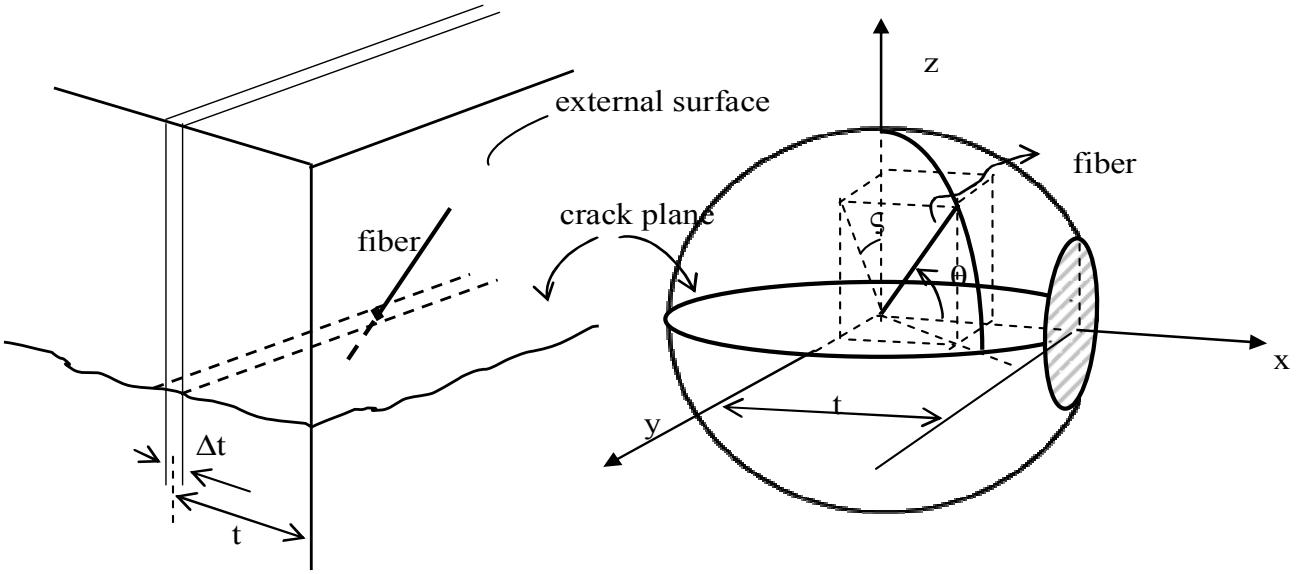

Figure 4. A slice is indicated parallel to the {*y,z*}-plane on a distance *t* from and parallel to the external surface of a prismatic FRC specimen. The leading crack is situated in the {*x,y*}-plane. A single fiber *intersecting the crack inside the slice* is shown. The angle enclosed by fiber and *x*-axis is θ, while the angle between the *z*-axis and the plane through the x-axis and the fiber

To this should be added how fiber numbers decline with *t/l* and over which part of the unit sphere the global geometric averaging process should be extended. Not particularly difficult, since one should only cope with elementary integrations in sine and cosine functions.

Of course, also the planar portion could be influenced by the mould. To transfer stresses over the crack, the orientation plane of the 2D portion is supposed perpendicular to the crack. Moreover, the orientation plane should also be perpendicular to the mould; when parallel to it, no decline in fiber reinforcement efficiency will occur. The linear portion only leads to trivial results, because when the orientation line is perpendicular to the crack, so that stresses are transferred, no decline will occur upon approach of the mould. In all other orthogonal cases, no stresses will be transferred.

Decline in the number of fibers per unit of crack area is plotted for the 3D and 2D fiber portions in Figure 5.This is a problem also discussed in (Soroushian 1990a,b); the plotted functions herein can be analytically integrated to represent arbitrarily thin SFRC elements.

The efficiency factor of the 3D portion is plotted in Figure 6 in accordance with the mathematical expression ($\cos\alpha = t/l$):

$$\eta_{b3} = \cos^3\alpha - 2\cos^2\alpha + 2\ln 2.\cos\alpha$$

$$\text{for} \qquad \frac{\pi}{3} \le \alpha \le \frac{\pi}{2} \qquad (12)$$

$$\eta_{b3} = -\frac{1}{3}\cos^3\alpha + 2\cos^2\alpha - \cos\alpha - 2\cos\alpha.\ln\cos\alpha - \frac{1}{3}$$

$$\text{for} \qquad 0 \le \alpha \le \frac{\pi}{3} \qquad (13)$$

The efficiency factor of the 2D portion is plotted in Figure 7 in accordance with the mathematical expression ($\cos\alpha = t/l$):

$$\eta_{b2} = \frac{2}{\pi}\{-\alpha - \frac{5}{2}\sin 2\alpha + \frac{\pi}{4} + 2\alpha\cos^2\alpha$$

$$+4\cos\alpha\ln tg(\frac{\alpha}{2} + \frac{\pi}{4})\} \quad (0 \le \alpha \le \frac{\pi}{3}) \qquad (14)$$

Since in general $V_{f3} >> V_{f2}$, we will neglect the *decline* of the 2D portion in the boundary zone. This leads to the total stress transfer capacity perpendicular to a crack with small opening due to a partially planar fiber system:

$$\sigma_x = \sigma_m(1-V_f) + \frac{1}{3}aV_f\tau_f(\bar{\eta}_{b3} + [\frac{1}{2} - \bar{\eta}_{b3}]\omega_2)$$

$$\approx \sigma_m(1-V_f) + 0.21aV_f\tau_f(1 + \frac{4}{3}\omega_2) \qquad (15)$$

in which ω_2 is the degree of orientation due to the planar portion as defined earlier. Further, $\bar{\eta}_{b3} = 0.213$. Hence, average efficiency of 3D fiber portion in a boundary zone of half the fiber length is 64% of that in bulk. When $\tau_f / \sigma_m \sim 1$ and 1% by volume of fibers with an aspect ratio of 100 is applied, the average strength reduction is of the order of 10%.

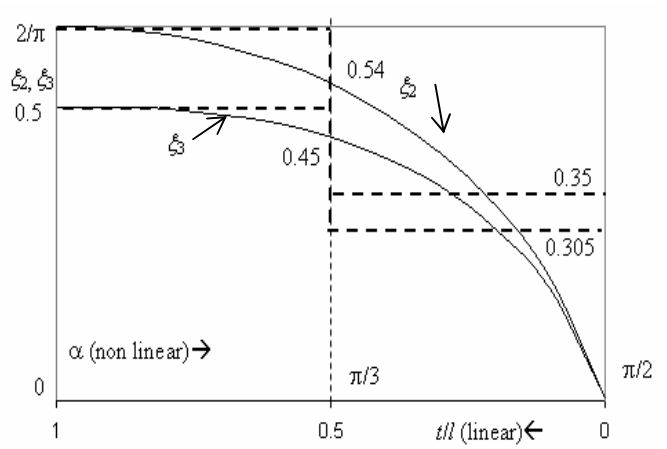

Figure 5. Decline in the number of fibers per unit of crack area for the 3D (ζ_3) and 2D (ζ_2) fiber portions in the boundary zone: $N_A(t/l)=\xi N_A(t>l)$.

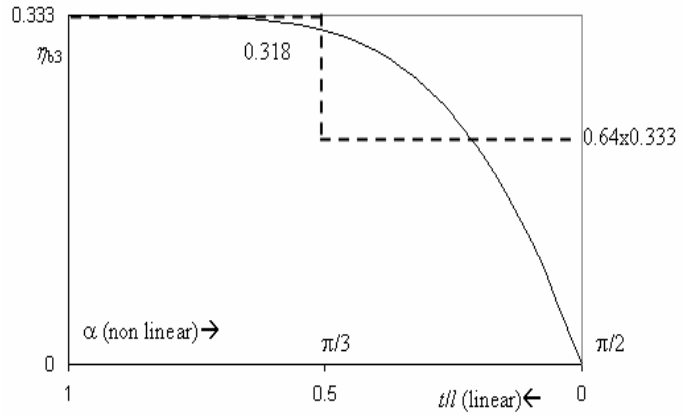

Figure 6. Decline towards the external boundary in the stress transfer capability of the 3D fiber portion (η_{b3}). Further, the average capacity is shown for a boundary zone of half the fiber length.

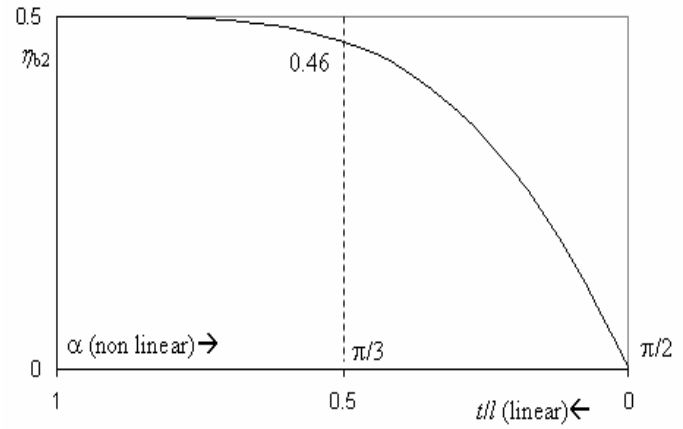

Figure 7. Decline towards the external boundary in the stress transfer capability of the 2D fiber portion (η_{b2}).

4 APPLICATION TO THIN PLATE

The 2D portion is not affected by the close proximity of the boundary when the orientation plane is parallel to this external surface (*i.e.,* crack perpendicular to top and bottom surfaces, respectively, in Fig.1). Hence, it will somewhat compensate for the strength loss in the boundary layer due to declined efficiency of the 3D portion. When the strength is considered at a side surface in *z*-direction (Fig. 1), so perpendicular to the orientation plane, and the crack is in the $\{x,y\}$-plane, the strength decline is at its maximum, since the 2D portion has no reinforcing effect (efficiency factor is nil). When the crack is perpendicular to the side surface (as in Fig. 4), and parallel to the other side surface, the strength (perpendicular to the crack) is somewhat affected by a decline in the 2D portion (but neglected in equation (15)) in addition to the reduction in the 3D portion. The first boundary effect is the relevant one when considering the first crack strength or ultimate tensile strength of thin fiber reinforced elements.

When the thickness of the structural element is h, bulk efficiency can be attributed to the central part (h-l). For the boundary zone (l), we have $(0.213V_{f3}+0.5V_{f2})a\tau_f=(0.213+0.287\omega_2)aV_f\tau_f$; for bulk $(0.333\ V_{f3}+0.5\ V_{f2})a\tau_f=(0.333+0.167\omega_2)aV_f\tau_f$. As a consequence, the tensile strength due to the fibers of the full section would be $[(0.333+0.167\omega_2) - 0.12(1-\omega_2)l/h]aV_f\tau_f$. Assume ω_2=0.1 (case 1), ω_2=0.2 (case 2) and ω_2=0.4 (case 3). This yields for the fiber efficiency factors, respectively:

$$\text{Case 1:}\quad \eta = 0.350 - 0.108\frac{l}{h} \tag{16}$$

$$\text{Case 2:}\quad \eta = 0.366 - 0.096\frac{l}{h} \tag{17}$$

$$\text{Case 3:}\quad \eta = 0.400 - 0.072\frac{l}{h} \tag{18}$$

The boundary zone extends over the full cross section for $h=l$; bulk properties are obtained for $h>>l$. Results are plotted in Figure 8. It should be noted that with a reduction in thickness of a plate from "thick" ($h>>l$) to "thin" ($h=l$), ω_2 will increase. N_A is according to Figure 5: $0.50L_{V3}+0.64L_{V2}$ and $0.305L_{V3}+0.64L_{V2}$ for $h>>l$ (bulk) and for $h=l$, respectively. By dividing both expressions, we find

$$\frac{N_A(h=l)}{N_A(h>>l)} = \frac{0.305+0.33\omega_2(h=l)}{0.50+0.14\omega_2(h>>l)} \tag{19}$$

Both parameters at the left as well as the degree of fiber orientation in bulk should be experimentally assessed. Let us assume that in bulk, ω_2=0.2. Further, 10% decline in the number of fibers per unit of area is assumed going from a "thick" to a "thin" plate. These values inserted in equation (19) yield ω_2=0.52 in the section at $h=l$. We see that from "thick" to "thin" plates, a very modest decline in the number of fibers per unit area in the section perpendicular to the tensile stress is accompanied by a dramatic increase in the degree of orientation. Going from a "thick" to a 'thin" plate leads according to Figure 8 to a slight decline in the fiber efficiency for constant degree of fiber orientation. This is in reality compensated for by the 2D portion taking to an increasing degree over from the less efficient 3D portion!

A similar modeling problem was also considered by Soroushian & Lee (1990b); they applied the results in Souroushian & Lee (1990a) to a thin SFRC element subjected to direct tension. *Orientation factors* were basically derived in accordance with the methodology outlined in this paper, however following the incorrect geometric averaging concept proposed by Romualdi & Mandel (1964). They incorporated orientation factors in the number of fibers per unit of area to account for the two wall effects, and found an acceptable correlation with tensile strength. Nevertheless, the orientation factors are fundamentally different from the efficiency factors developed herein. Compare therefore Figures 5-7.

3D and 2D orientation factors are long proven to be 1/2 and 2/π (Stroeven 2009, Stroeven & Hu 2006, Aveston & Kelly 1973), whereas efficiency factors are 1/3 and 1/2, respectively (all in bulk). So, ratios of orientation over efficiency factors are for the respective portions 3/2 and 4/π, not allowing for a linear transformation of their data. Hence, their graphs of orientation factor versus relative thickness of the SFRC element run similarly as in Figure 8 but at higher values outside the picture.

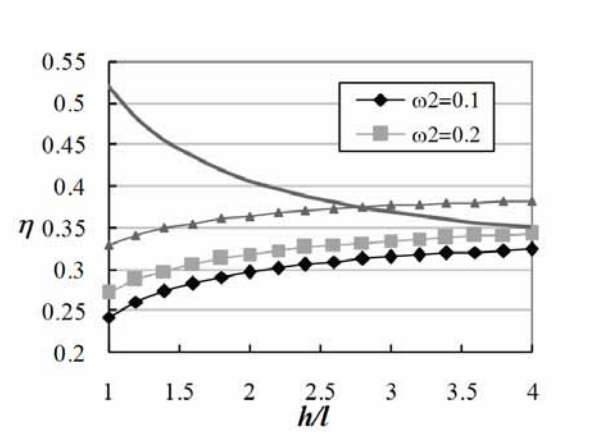

Figure 8. In-plane fiber efficiency in a thin SFRC element subjected to tensile stresses. Reinforcement efficiency is presented as function of the element's relative thickness (so, only top and bottom surfaces are supposed to influence fiber efficiency) and the degree of fiber orientation. The latter will increase for thinner elements (should be experimentally assessed); this is illustrated by the thick black line.

From such a correlation between incorrectly interpreted efficiency data and tensile strength values for a thin SFRC element they conclude that an average could be taken of 2D and 3D solutions. This crude approximation is however not necessary, since the mathematically exact solutions given in this paper (based on Stroeven 2009, Stroeven & Hu 2006) prevent the need to do so. Moreover, the Stroeven concept already assumes a *mixture* of 2D and 3D portions, however adapted to the situation at issue by experimental assessment of the ratio of 3D and 2D components.

5 CONCLUSIONS

The intersection of an active fiber and the crack is a probability event. The associated probability factor is proportional to the fiber's tangent height (projected length perpendicular to the crack $=\cos\theta$, with θ as the angle enclosed by loading direction and fiber). Spatial averaging of all possible fiber orientations requires doing so over an angle in the crack plane and over the sine value of another independent angle ($=\sin\theta$). Spatial averaging in all modeling efforts should be in accordance with this scientific framework. So, an IUR ("random") fiber system in bulk (the common assumption) yields active fibers reinforcing the crack that are distributed according to a $\sin 2\theta$ function with respect to crack plane or loading axis. Hence, active fibers can never be distributed "randomly" as frequently adopted.

These established stereological principles are employed in modeling of fibers in bulk and boundary zones. Orthogonal efficiency factors are readily obtained for 1D, 2D and 3D fiber portions that are combined to constitute the efficiency concept for the partially linear planar "Stroeven" system. The decline over the boundary zone in fiber efficiency of 2D and 3D portions, resulting from external compaction by vibration of the fresh concrete, is derived applying a similar methodological strategy. An effective system is obtained for approaching practical problems. It is demonstrated functional in expressing the fiber efficiency in a tensile test of a thin plate. The resulting relationships of fiber efficiency in the plane of the element versus relative thickness of the element and degree of fiber orientation reveal the approach more accurate than a pragmatic approach available in the international literature.

REFERENCES

Aveston, J. & Kelly, A. 1973. Theory of multiple fracture of fibrous composites. *Journal of Materials Science* 8(3): 352-362.

Bayard, O. et al. 2004. Internal heterogeneity in a reactive powder concrete. In M. di Prisco, R. Felicetti & G.A. Plizzari (eds), *Fiber Reinforced Concretes*, Proceedings *BEFIB*: 61-68. Bagneux: RILEM Publications S.A.R.L.

Bentur, A. & Mindess, S. 1990. *Fiber reinforced cementitious composites*. New York: Elsevier Appl. Sc.

Bonzel, J. & Schmidt, M. 1985. Verteilung und Orientierung von Stahlfasern im Beton und ihr Einfluss auf Eigenschaften von Stahlfaserbeton. *Beton* (in Germany) 11: 463-470 and 12: 501-504.

Gettu, R., Gardner, D.R., Saldívar, H. & Barragán, B.E. 2005. Study of the distribution and orientation of fibers in SFRC specimens. *Materials and Structures* 38(275): 31-37.

Romualdi, J.P. & Mandel, J.A. 1964. Tensile strength of concrete affected by uniformly distributed and closely spaced short lengths of wire reinforcement. *Journal of the American Concrete Institute* 61(6): 657:671.

Soroushian, P. & Lee, C-D. 1990a. Tensile strength of fiber reinforced concrete: correlation with some measures of fiber spacing. *American Concrete Institute Materials Journal* 87(6): 541-546

Soroushian, P. & Lee, C-D. 1990b. Distribution and orientation of fibers in steel fiber reinforced concrete, *American Concrete Institute Materials Journal* 87(5): 433-439.

Stroeven, P. & Babut, R. 1986. Fracture mechanics and structural aspects of concrete, *Heron* 31(2): 15-44.

Stroeven, P. & Guo, Z. 2008. Distribution and orientation of fibers in the perspective of the mechanical properties of concrete, In R. Gettu (ed.), *Proceedings of the 7th International RILEM-Symposium on Fibre Reinforced Concrete: Design and Applications BEFIB 2008*:145-154. Bagneux: RILEM Publications S.A.R.L.

Stroeven, P. & Hu, J. 2006. Effectiveness near boundaries of fibre reinforcement in concrete. *Materials and Structures* 39: 1001-1013.

Stroeven, P. & Shah, S.P. 1978. Use of radiography-image analysis for steel fiber reinforced concrete. In R.N. Swamy (ed.): 345-353. *Testing and Test Methods of Fiber Cement Composites*, Lancaster: Construction Press.

Stroeven, P. 1979a. Micro- and macromechanical behaviour of steel fiber reinforced mortar in tension, *Heron* 24(4): 7-40.

Stroeven, P. 1979b. Morphometry of fiber reinforced cementitious materials (part II), *Materials and Structures* 12(67): 9-20.

Stroeven, P. 1989. Discussion on Behavior of reinforced steel-fiber-concrete beams in flexure by Lim T-Y, *et al. Journal of Structural Engineering, American Society Civil Engineers Structural Division*, 115(7): 1825-1827.

Stroeven, P. 2009. Stereological principles of spatial modeling applied to steel fiber-reinforced concrete in tension. *American Concrete Institute Materials Journal* 106(3): 213-222.

Yamada, K. & Ishiyama, S. 2004. Determination of fiber contribution in composites employing tension softening properties", In M. di Prisco, R. Felicetti & G.A. Plizzari (eds): 443-452. *Fiber Reinforced Concretes*, *Proceedings BEFIB 2004*. Bagneux: RILEM Publications S.A.R.L.